The decadal variation in displacement sudden stratospheric warmings driven by Pacific teleconnections

Yuanpu Li[1*] and Zhiping Wen[1*]

1 Institute of Atmospheric Sciences, Fudan University, Shanghai, China

*Corresponding author:

Yuanpu Li (liyuanpu@fudan.edu.cn)

ORCID: https://orcid.org/0000-0003-3047-5675

Zhiping Wen (zpwen@fudan.edu.cn)

ORCID: https://orcid.org/0000-0003-0178-9835

Key Points:

Main point #1:

A new index describing the combined impact of PNA and WP is defined to explain the decadal variation in SSWs.

Main point #2:

+PNA+WP and -PNA-WP have an essential role in modulating planetary wave 1 and displacement SSWs.

Main point #3:

The second mode of tropical Pacific SST modulates the decadal variation in PWC Index and displacement SSWs.

Abstract

Sudden stratospheric warmings (SSWs) are important processes that exert impacts on tropospheric weather and climate. This study used the duration to describe the variations in the displacement SSWs and defined Pacific–North American (PNA) and Western Pacific (WP) combined indices (PWC Index) to describe the combinations of PNA and WP. We found that the duration of the displacement SSWs (SSW1) first increased and then decreased around 2000. The decadal variation in SSW1 can be explained by PWC Index, since the teleconnection combinations with the same signs (+PNA+WP/−PNA−WP) can affect upward planetary wave 1 and SSW1 more efficiently than +PNA−WP/−PNA+WP. The second mode of tropical Pacific sea surface temperature plays a more important role in modulating the decadal variations in PWC Index and displacement SSWs than the first mode.

Plain Language Summary

The low-frequency variation in SSWs can effectively modulate the tropospheric climate change, which highlights the importance of studying the decadal variation in SSWs. However, it is unclear if the low-frequency variations in SSWs occur by chance or due to external factors. Both individual Pacific-North America (PNA) and Western Pacific (WP) teleconnection can affect SSWs, but there is no index to describe the combined impact of PNA and WP on SSWs. This study used the coordinate rotation method to define PNA and WP combined indices (PWC Index). We found that the decadal variation in the duration of displacement SSWs is consistent with that in the combinations of PNA and WP. The second principal component of the Pacific sea surface temperature also plays essential roles in modulating the decadal variations in the teleconnections and SSWs. The potential application of PWC Index may be extended to on other tropospheric climate change.

Keywords: teleconnection; sudden stratospheric warmings; decadal variation

Introduction

Sudden stratospheric warmings (SSWs) are rapid temperature-rising processes that occur in the polar stratosphere in winter. During SSW, the mid-to-upper stratosphere in the polar region rises by more than 40 K in a few days (*Butler et al.*, 2015). Weak polar vortex events or SSWs are related to the negative North Atlantic Oscillation or Arctic Oscillation anomalies and southward shift of storm tracks in Europe (*Baldwin and Dunkerton*, 2001; *Baldwin et al.*, 2021; *Polvani et al.*, 2017). Just as many strong warmings had an important effect on the troposphere, some minor warmings (*Domeisen and Butler*, 2020; *Hendon et al.*, 2019; *Lim et al.*, 2019; *Rao et al.*, 2020; *Wang and Chen*, 2010) were related to the tropospheric weather anomalies. SSWs in this study include both major and minor SSWs. SSWs can be classified into two types: vortex-displacement and vortex-splitting (*Charlton and Polvani*, 2007). These types of SSWs have different impacts on the troposphere (*White et al.*, 2021). The vortex-displacement SSWs are mostly preceded by planetary wave 1 (PW1) anomalies, while vortex-splitting SSWs are preceded by either PW1 or planetary wave 2 (PW2) anomalies (*Ayarzagüena et al.*, 2019; *Bancalá et al.*, 2012; *Barriopedro and Calvo*, 2014; *Smith and Kushner*, 2012). The SSWs preceded by PW1 forcing are abbreviated as SSW1, and the SSWs preceded by PW2 anomalies are abbreviated as SSW2. The low-frequency variation in SSWs can effectively modulate the Atlantic Meridional Overturning Circulation (*Reichler et al.*, 2012), which highlights the importance of studying the decadal-scale variation in SSWs. However, it is unclear if the decadal-scale variability of SSWs occurred by chance or

partially due to external factors such as oceanic variability (*Baldwin et al.*, 2021).

The Pacific–North American (PNA) teleconnection and Western Pacific (WP) teleconnection are the two dominant tropospheric modes in the Pacific winter (*Linkin and Nigam*, 2008). Both teleconnections effectively interfere with the low height center over the subpolar North Pacific, which is a key region to trigger SSWs (*Garfinkel et al.*, 2010; *Garfinkel et al.*, 2012). Therefore, the PNA and WP teleconnections are good precursors of SSWs and they can jointly affect SSWs (*Bao et al.*, 2017; *Dai and Tan*, 2016). Previous studies have found that though PNA and WP are the atmospheric internal dynamic variabilities, they are modulated by tropical and extratropical Pacific SST (*e.g., Dai and Tan,* 2019*; Hu and Guan,* 2018; *Hu et al.,* 2021; *Hurwitz et al.,* 2012; *Li et al.,* 2019; *Liu et al.,* 2020; *Straus and Shukla,* 2000; 2002).

The forcing associated with the Pacific sea surface temperature (SST) plays an important role in modulating SSWs. El Niño-Southern Oscillation (ENSO) is the leading mode of SST in the tropical Pacific (*Feng et al.*, 2020). El Niño-related tropical forcing induces more upward Rossby wave propagation into the stratosphere and a weakened vortex, while La Niña induces a general opposite process to El Niño (*Barriopedro and Calvo*, 2014; *Garfinkel and Hartmann*, 2008; *Li and Lau*, 2013). However, over the past 40 years, there have been more SSWs in La Niña than El Niño (*Domeisen et al.*, 2019). There is less consensus regarding whether Modoki El Niño weakens the stratospheric polar vortex (*Calvo et al.*, 2017; *Domeisen et al.*, 2019; *Garfinkel et al.*, 2013; *Xie et al.*, 2012). The impact of Modoki La Niña (MLN) on

SSW has received less attention because the response of the Arctic stratosphere to La Niña is relatively weak compared to El Niño (*Xie et al.*, 2018).

This study proposed a new index to describe the combined impact of PNA and WP, which can explain the decadal variation in the displacement SSWs. The origin of the decadal variation in the combinations of PNA and WP is attributed to the second mode of tropical Pacific SST.

Data and Methods

ERA5 (*Hersbach et al.*, 2020) and NCEP (*Kalnay et al.*, 1996), and JRA55 (*Kobayashi et al.*, 2015) reanalysis provided geopotential height, wind, and temperature data. HadISST (*Rayner et al.*, 2003) provided SST data.

Definitions of the climate indices

PNA and WP indices. The PNA and WP are defined by the modified pointwise method, which is proposed by Climate Prediction Center of NOAA. (https://www.cpc.ncep.noaa.gov/products/precip/CWlink/pna/month_pna_index2.shtml; https://psl.noaa.gov/data/timeseries/daily/WPO/).

PWC Index. PNA and WP combined indices (PWC Index) are obtained by rotating the coordinate axes, which is illustrated in Fig. 1a. Since the correlation coefficient between PNA and WP in 1979-2020 is 0.03, the two indices can be considered orthogonal. Any year can be represented as a point in a Cartesian coordinate system with the PNA and WP indices as the black axes. Then rotate the coordinate axes 45° to the right to get the red coordinate axes. The value of any point projected onto the

first axis is defined as **PWC1**, and the value projected onto the second axis is defined as **PWC2**. The formula for projection is as follows:

$$PWC1 = \frac{\sqrt{2}}{2}PNA + \frac{\sqrt{2}}{2}WP$$
$$PWC2 = \frac{\sqrt{2}}{2}PNA - \frac{\sqrt{2}}{2}WP$$

The newly obtained indices are continuous scalar (shown in Fig. 1b). A positive PWC1 indicates a feature with +PNA+WP, and a negative PWC1 indicates a feature with -PNA-WP. A positive PWC2 indicates a feature with +PNA-WP, and a negative PWC2 indicates a feature with -PNA+WP.

+PNA+WP/−PNA−WP index. If winter has positive PNA and positive WP index, then the winter is assigned with a value of +1. If winter has negative PNA and negative WP index, then the winter is assigned with a value of -1.

+PNA−WP/−PNA+WP index. If winter has a positive PNA and negative WP index, then the winter is assigned with a value of +1. If winter has a negative PNA and positive WP index, then the winter is assigned with a value of −1.

SSWs. SSWs are defined when the daily temperature gradient between 60°N and 90°N at 10 hPa becomes positive, including both minor and major warmings. Only warmings during December–February are counted.

SSW duration. SSWs were classified into wave-1 and wave-2 events according to the method proposed by *Barriopedro and Calvo* (2014). We defined Z1 and Z2 as the daily amplitudes of PW1 and PW2 in geopotential height at 50 hPa, 60°N obtained by Fourier decomposition.

If a day from December to February satisfies the following criterion, then this day is

added to **SSW1 duration**: the gradient of temperature between 60°N and 90°N at 10 hPa at this day becomes positive; Z2−Z1 < 200 m is satisfied for the entire previous 10 days before this day, and [Z2] < [Z1] (the brackets denote the averaged amplitude of Z1 and Z2 of the previous 10 days).

If a day from December to February satisfies the following criterion, then this day is added to **SSW2 duration**: the gradient of temperature between 60°N and 90°N at 10 hPa at this day becomes positive; Z2−Z1 ≥ 200 m persists for more than 1 day within the 10 days before this day, or [Z2] ≥ [Z1]. The total numbers of SSW1 and SSW2 days in the winter (December−February) are the duration of SSW1 and SSW2.

The Eliassen-Palm (EP) flux and its divergence are calculated using the same method introduced by *Andrews et al.* (1987).

SST-PC1 and SST-PC2. The December to February SST fields were detrended, and then EOF analysis is exerted on SST over the domain of 30°S–30°N, 120°E–100°W to distinguish the two main modes.

Statistics

A Monte Carlo test has been adopted to determine the statistical significance of the deviations from climatology during different teleconnection combinations (Fig. 4). We randomly subsampled elements from all winters and averaged the result. The number of sub-samples matches the number of each teleconnection combination. We repeated this random selection process 1,000,000 times to obtain a probability density function. The significance of the deviation was estimated using the density function.

The consistency of SSW1 and PWC1

The duration of SSW1 experienced a decadal-scale variation that reached a peak around 2003 (Fig. 2e), while the duration of SSW2 had no obvious decadal-scale changes since 1979. Past studies documented that the frequency of major SSWs had experienced decadal-scale variation. *Reichler et al.*, (2012) showed the peak of the moving average of major SSWs was reached around 1995. *Butler et al.* (2017) have pointed there were relatively more SSWs in the 2000s than in the 1990s. PWC1 has a similar decadal variation as SSW1, and the correlation coefficient of the moving average of the two climate indices is 0.9 (Table 1). The decadal variation in PWC2 is not consistent with that in SSW1. The correlation between PWC1 and SSW1 is higher than the correlation between single PNA or WP and SSW1, no matter on the interannual or decadal scale. Fig. 2a and 2b show binary indices to describe the combinations of PNA and WP. The results in Fig. 2a and 2b are obtained by dividing the phases of PNA and WP with 0 as the threshold. If other threshold values are used, the decadal variation curve of +PNA+WP/−PNA−WP will not change significantly. The 11-year moving average of +PNA+WP/−PNA−WP is consistent with that of PWC1. The binary indices are convenient to facilitate composite analysis, thus the composite results of Fig. 3 and 4 are based on Fig. 2a and 2b. The consistency among the moving averages of SSW1, PWC1, +PNA+WP/−PNA−WP implies the decadal variation in the displacement SSWs originates from the decadal change in the combined effects of PNA and WP.

The SSW1 also have a higher positive correlation with PWC1 than PWC2, single

194 PNA or WP index on interannual scale (Table 1). This indicates that the decadal-scale
195 consistency of SSW1 and PWC1 is based on the mechanism of interannual-scale
196 connection between them. Figure 3a shows that the centers of the PW1 component of
197 the height anomalies during +PNA+WP are in-phase with the climatological pattern
198 of PW1. This pattern implies a strengthened PW1 in the upper troposphere and
199 opposite for −PNA−WP. The anomalous centers of +PNA−WP and −PNA+WP are
200 not overlapped with the climatological centers, and their anomalies are smaller than
201 those of +PNA+WP and −PNA−WP. Therefore, the impacts of +PNA−WP and
202 −PNA+WP on the PW1 are smaller than those of +PNA+WP and −PNA−WP. During
203 +PNA+WP pattern, PW1 propagating to the stratosphere has increased significantly,
204 accompanied by the convergence of EP fluxes in the polar stratosphere. During
205 −PNA−WP pattern, PW1 propagating to the stratosphere has reduced significantly,
206 accompanied by the divergence of EP fluxes in the polar stratosphere. +PNA−WP and
207 −PNA+WP have little effect on upward propagating of PW1 (Fig. 3c). The PW2
208 anomalies of +PNA+WP are in disagreement with climatology PW2, whereas those
209 of −PNA−WP are in agreement with climatology PW2 (Fig. 3b). There are more (less)
210 PW2 EP fluxes propagating to the stratosphere during −PNA−WP (+PNA+WP) (Fig.
211 3d). This explains why PWC1 is negatively correlated with the duration of SSW2 on
212 an interannual scale.

213 The SSW1 duration appears longer (shorter) during +PNA+WP (−PNA−WP),
214 corresponding to the significant enhancement (weakening) of PW1 propagated to the
215 stratosphere. The deviations of SSW1 duration of +PNA−WP and −PNA+WP from

the climatology are negligible (Fig. 4a). For the duration of SSW2, only +PNA+WP and −PNA+WP statistically significantly deviate from the climatology (Fig. 4b). Yet, the anomalies in SSW2 duration during −PNA+WP are challenging to explain from divergence of PW2. During the analysis of distribution of a major SSW duration, we use ERA5 and NCEP from 1950 to 2020 and JRA55 from 1958 to 2020 since winters without major SSWs appear very frequently during these years and longer data record ensures the robustness of the results. The distribution of major SSW duration in different teleconnection combinations is consistent with the distribution of SSW duration.

The Pacific SST origin of the decadal variation in PWC1

The first two principal components derived from empirical orthogonal function **(**EOF) analysis on the winter tropical Pacific SST (30°S–30°N) are shown in Fig. 2f. The regressed SST anomalies of the first principal component (SST-PC1) corresponds to Eastern Pacific El Niño (EEN) with a dipole pattern (Fig. 5c), while the regressed SST anomalies of the second principal component (SST-PC2) resemble Modoki La Niña (MLN) with a tripole pattern (Fig. 5d) (*Ashok and Yamagata*, 2009; *Feng et al.*, 2020). The regressed SST anomalies of PWC1 (Fig. 5b) also have a tripole pattern similar to SST-PC2, while the regressed SST anomalies of PWC2 (Fig. 5a) have a dipole pattern similar to SST-PC1. The interannual correlation coefficients show that PWC1 is strongly related to SST-PC2, while PWC2 is more related to SST-PC1. The correlation coefficients of the moving averaged indices show that the decadal

238 variation in SST-PC2 is more consistent with that in PWC1 than in SST-PC1 (also see
239 Fig. 2e).

240 Previous studies have pointed out that different modes of tropical and
241 extratropical SST anomalies can modulate PNA (*Johnson and Feldstein*, 2010) and
242 WP (*Dai and Tan*, 2016; *Furtado et al.*, 2012; *Liu et al.,* 2020; *Hu et al.,* 2021). There
243 are positive SST anomalies in the eastern and western boundary of the tropical Pacific
244 in the pattern of SST-PC2. The warming from 150°W to 110°W is located over the
245 region where the climatology of the SST is above 25°C and above the threshold for
246 convection to trigger (*Johnson and Xie*, 2010). The warming in this region causes Gill
247 response (*Gill*, 1980), an anticyclone pair propagating Rossby waves northward to the
248 extratropical Pacific. Therefore, the positive SST anomalies in the eastern Pacific
249 favor the occurrence of +PNA (*Horel and Wallace*, 1981; *Li and Wen*, 2021). The
250 warming of tropical eastern Pacific SST can promote the evolution of the synoptic-
251 scale +PNA anomalies into +WP anomalies (*Dai and Tan*, 2016). Moreover, when the
252 western Pacific boundary current tends to be warmer, +WP is more likely to emerge
253 (*Li et al.*, 2018; *Hu et al.,* 2021). *Hurwitz et al.,* (2012) performed two sets of
254 sensitivity experiments using fixed North Pacific (north of 20°N) SST boundary
255 conditions. The pattern of the differences in SST between the two experiment sets
256 (Fig. 1d in *Hurwitz et al.,* 2012) is similar to the regressed SST anomalies to SST-PC2
257 (north of 20°N) (the signs of anomalies are opposite). Their result implies that the
258 associated extratropical Pacific SST with SST-PC2 contributes to the enhancement of
259 +WP. However, the understanding of the evolution of WP is less comprehensive than

that of PNA (*Dai and Tan,* 2019). The relationship between SST and WP needs further research in the future.

Summary and discussion

Based on previous studies, this study used SSW duration to study the decadal variation in the displacement SSWs and proposed a new PWC Index to describe the joint impact of PNA and WP. Although the frequencies of SSWs in some winters are the same, the differences in the duration reflect more information about SSWs, which is helpful to find the factors that affect the interannual and decadal variation in SSWs through correlation analysis. PWC Indices are continuous scalar indices, which include the year-to-year differences in the PNA and WP combinations, bringing convenience to correlation analysis. This study found that PWC1 or +PNA+WP/−PNA−WP could explain the decadal variation in the displacement SSWs.

This study suggested SST-PC2 is the origin of the decadal variation in PWC1, in which both tropical and extratropical SST anomalies related to SST-PC2 could contribute to the change of PNA and WP. SST-PC2 first regulates PWC1, and then, PWC1 affects the SSW1. On the interannual scale, SST-PC2 and SSW1 have a positive correlation, in other words, positive SST-PC2 (corresponding to Modoki La Niña; based on Ashok and Yamagata, 2009) favors the occurrence of SSW1, while negative SST-PC2 (corresponding to Modoki El Niño) is unfavorable for the occurrence of SSW1. *Hegyi and Deng* (2011) and Xie *et al.*, (2019) also stated that

Modoki El Niño leads to a strengthened vortex (fewer SSWs occur). The interannual correlation coefficients show that SST-PC1 has a more significant impact on SSW1 than SST-PC2. However, the decadal variation in SSW1 is more consistent with SST-PC2 rather than SST-PC1. It is still not fully understood to what extent ENSO diversity affects SSWs (*Domeisen et al.*, 2019). Previous studies on Modoki ENSO also have found that it is difficult to objectively define Modoki La Niña separate from canonical La Niña, as there is less inter-event diversity in the SST pattern for La Niña events (Garfinkel et al 2013; Capotondi et al 2015). The stratospheric response is also sensitive to different indices describing Modoki ENSO (Garfinkel et al 2013). Therefore, although we found the relationship between SST-PC2 and SSW1, we are cautious to use the expression that Modoki La Niña favors SSW1.

The PNA and WP teleconnections are the internal variabilities of the atmosphere. There are mutual feedbacks between the tropical ocean and the extratropical atmosphere teleconnection because North Pacific Oscillation or WP variation can also modulate the SST-PC2 through the Pacific meridional mode (Fig. 3 in *Di Lorenzo et al.,* 2015). It is challenging to separate the cause-and-effect relationship of the SST-PC2 and PWC1. Although the decadal changes in Pacific SST and teleconnections are not independent of each other, both of they are the origins of the decadal variations in the displacement SSWs.

Acknowledgments

This work was supported jointly by the National Natural Science Foundation of China

(41805029, 41875087, 42030601) and China Postdoctoral Science Foundation (2018M641913). Thanks to the two anonymous reviewers for their valuable advices.

Open Research

Data Availability Statement

ERA5, NCEP, JRA55 and HadISST are publicly available on the following websites.

ERA5: https://doi.org/10.24381/cds.bd0915c6

NCEP: https://psl.noaa.gov/data/gridded/data.ncep.reanalysis.html

JRA55: https://doi.org/10.5065/D6HH6H41

HadISST: https://www.metoffice.gov.uk/hadobs/hadisst/data/download.html

Competing interests

The Authors declare no Competing Financial or Non-Financial Interests.

References

Andrews, D. G., J. R. Holton, and C. B. Leovy (1987), Middle atmosphere dynamics, Academic press.

Ashok, K., and T. Yamagata (2009), The El Niño with a difference, Nature, 461(7263), 481-484.

Ayarzagüena, B., F. M. Palmeiro, D. Barriopedro, N. Calvo, U. Langematz, and K. Shibata (2019), On the representation of major stratospheric warmings in reanalyses, Atmos.

326 Chem. Phys., 19(14), 9469-9484.
327 Baldwin, M. P., and T. J. Dunkerton (2001), Stratospheric Harbingers of Anomalous Weather
328 Regimes, Science, 294(5542), 581-584.
329 Baldwin, M. P., et al. (2021), Sudden Stratospheric Warmings, Reviews of Geophysics, 59(1),
330 e2020RG000708.
331 Bancalá, S., K. Krüger, and M. Giorgetta (2012), The preconditioning of major sudden
332 stratospheric warmings, Journal of Geophysical Research: Atmospheres, 117(D4).
333 Bao, M., X. Tan, D. L. Hartmann, and P. Ceppi (2017), Classifying the tropospheric precursor
334 patterns of sudden stratospheric warmings, Geophysical Research Letters, 44(15), 8011-
335 8016.
336 Barriopedro, D., and N. Calvo (2014), On the Relationship between ENSO, Stratospheric
337 Sudden Warmings, and Blocking, Journal of Climate, 27(12), 4704-4720.
338 Butler, A. H., J. P. Sjoberg, D. J. Seidel, and K. H. Rosenlof (2017), A sudden stratospheric
339 warming compendium, Earth Syst. Sci. Data, 9(1), 63-76.
340 Butler, A. H., D. J. Seidel, S. C. Hardiman, N. Butchart, T. Birner, and A. Match (2015),
341 Defining Sudden Stratospheric Warmings, Bulletin of the American Meteorological
342 Society, 96(11), 1913-1928.
343 Calvo, N., M. Iza, M. M. Hurwitz, E. Manzini, C. Peña-Ortiz, A. H. Butler, C. Cagnazzo, S.
344 Ineson, and C. I. Garfinkel (2017), Northern Hemisphere Stratospheric Pathway of
345 Different El Niño Flavors in Stratosphere-Resolving CMIP5 Models, Journal of Climate,
346 30(12), 4351-4371.
347 Capotondi, A., et al. (2015), Understanding ENSO Diversity, Bulletin of the American

348 Meteorological Society, 96(6), 921-938.
349 Charlton, A. J., and L. M. Polvani (2007), A New Look at Stratospheric Sudden Warmings.
350 Part I: Climatology and Modeling Benchmarks, Journal of Climate, 20(3), 449-469.
351 Dai, Y., and B. Tan (2016), The western Pacific pattern precursor of major stratospheric
352 sudden warmings and the ENSO modulation, Environmental Research Letters, 11(12),
353 124032.
354 Dai, Y., and B. Tan (2019), Two Types of the Western Pacific Pattern, Their Climate Impacts,
355 and the ENSO Modulations, Journal of Climate, 32(3), 823-841.
356 Di Lorenzo, E., G. Liguori, N. Schneider, J. C. Furtado, B. T. Anderson, and M. A. Alexander
357 (2015), ENSO and meridional modes: A null hypothesis for Pacific climate variability,
358 Geophysical Research Letters, 42(21), 9440-9448.
359 Domeisen, D. I. V., and A. H. Butler (2020), Stratospheric drivers of extreme events at the
360 Earth's surface, Communications Earth & Environment, 1(1), 59.
361 Domeisen, D. I. V., C. I. Garfinkel, and A. H. Butler (2019), The Teleconnection of El Niño
362 Southern Oscillation to the Stratosphere, Reviews of Geophysics, 57(1), 5-47.
363 Feng, Y., X. Chen, and K.-K. Tung (2020), ENSO diversity and the recent appearance of
364 Central Pacific ENSO, Climate Dynamics, 54(1), 413-433.
365 Furtado, J. C., E. Di Lorenzo, B. T. Anderson, and N. Schneider (2012), Linkages between
366 the North Pacific Oscillation and central tropical Pacific SSTs at low frequencies, Climate
367 Dynamics, 39(12), 2833-2846.
368 Garfinkel, C. I., and D. L. Hartmann (2008), Different ENSO teleconnections and their effects
369 on the stratospheric polar vortex, Journal of Geophysical Research: Atmospheres,

113(D18).

Garfinkel, C. I., D. L. Hartmann, and F. Sassi (2010), Tropospheric Precursors of Anomalous Northern Hemisphere Stratospheric Polar Vortices, Journal of Climate, 23(12), 3282-3299.

Garfinkel, C. I., M. M. Hurwitz, D. W. Waugh, and A. H. Butler (2013), Are the teleconnections of Central Pacific and Eastern Pacific El Niño distinct in boreal wintertime?, Climate Dynamics, 41(7), 1835-1852.

Garfinkel, C. I., A. H. Butler, D. W. Waugh, M. M. Hurwitz, and L. M. Polvani (2012), Why might stratospheric sudden warmings occur with similar frequency in El Niño and La Niña winters?, Journal of Geophysical Research: Atmospheres, 117(D19).

Gill, A. E. (1980), Some simple solutions for heat-induced tropical circulation, Quarterly Journal of the Royal Meteorological Society, 106(449), 447-462.

Hegyi, B. M., and Y. Deng (2011), A dynamical fingerprint of tropical Pacific sea surface temperatures on the decadal-scale variability of cool-season Arctic precipitation, Journal of Geophysical Research: Atmospheres, 116(D20).

Hendon, H. H., et al. (2019), Rare forecasted climate event under way in the Southern Hemisphere, Nature, 573(7775), 495.

Hersbach, H., et al. (2020), The ERA5 global reanalysis, Quarterly Journal of the Royal Meteorological Society, 146(730), 1999-2049.

Horel, J. D., and J. M. Wallace (1981), Planetary-Scale Atmospheric Phenomena Associated with the Southern Oscillation, Monthly Weather Review, 109(4), 813-829.

Hu, D., and Z. Guan (2018), Decadal Relationship between the Stratospheric Arctic Vortex

392 and Pacific Decadal Oscillation, Journal of Climate, 31(9), 3371-3386.
393 Hu, D., Z. Guan, M. Liu, and W. Feng (2021), Dynamical mechanisms for the recent ozone
394 depletion in the Arctic stratosphere linked to North Pacific sea surface temperatures,
395 Climate Dynamics.
396 Hurwitz, M. M., P. A. Newman, and C. I. Garfinkel (2012), On the influence of North Pacific
397 sea surface temperature on the Arctic winter climate, J. Geophys. Res., 117, D19110.
398 Johnson, N. C., and S.-P. Xie (2010), Changes in the sea surface temperature threshold for
399 tropical convection, Nature Geoscience, 3(12), 842-845.
400 Johnson, N. C., and S. B. Feldstein (2010), The Continuum of North Pacific Sea Level
401 Pressure Patterns: Intraseasonal, Interannual, and Interdecadal Variability, Journal of
402 Climate, 23(4), 851-867.
403 Kalnay, E., et al. (1996), The NCEP/NCAR 40-Year Reanalysis Project, Bulletin of the
404 American Meteorological Society, 77(3), 437-472.
405 Kobayashi, S., et al. (2015), The JRA-55 Reanalysis: General Specifications and Basic
406 Characteristics, Journal of the Meteorological Society of Japan. Ser. II, 93(1), 5-48.
407 Li, X., Z.-Z. Hu, P. Liang, and J. Zhu (2019), Contrastive Influence of ENSO and PNA on
408 Variability and Predictability of North American Winter Precipitation, Journal of Climate,
409 32(19), 6271-6284.
410 Li, Y., and N.-C. Lau (2013), Influences of ENSO on Stratospheric Variability, and the
411 Descent of Stratospheric Perturbations into the Lower Troposphere, Journal of Climate,
412 26(13), 4725-4748.
413 Li, Y., and Z. Wen (2021), Influence of tropical convective enhancement in Pacific on the

trend of stratospheric sudden warmings in Northern Hemisphere, Climate Dynamics.

Li, Y., W. Tian, F. Xie, Z. Wen, J. Zhang, D. Hu, and Y. Han (2018), The connection between the second leading mode of the winter North Pacific sea surface temperature anomalies and stratospheric sudden warming events, Climate Dynamics, 51(1), 581-595.

Lim, E.-P., H. H. Hendon, G. Boschat, D. Hudson, D. W. J. Thompson, A. J. Dowdy, and J. M. Arblaster (2019), Australian hot and dry extremes induced by weakenings of the stratospheric polar vortex, Nature Geoscience, 12(11), 896-901.

Linkin, M. E., and S. Nigam (2008), The North Pacific Oscillation–West Pacific Teleconnection Pattern: Mature-Phase Structure and Winter Impacts, Journal of Climate, 21(9), 1979-1997.

Liu, M., D. Hu, and F. Zhang (2020), Connections Between Stratospheric Ozone Concentrations Over the Arctic and Sea Surface Temperatures in the North Pacific, Journal of Geophysical Research: Atmospheres, 125(4), e2019JD031690.

Polvani, L. M., L. Sun, A. H. Butler, J. H. Richter, and C. Deser (2017), Distinguishing Stratospheric Sudden Warmings from ENSO as Key Drivers of Wintertime Climate Variability over the North Atlantic and Eurasia, Journal of Climate, 30(6), 1959-1969.

Rao, J., C. I. Garfinkel, I. P. White, and C. Schwartz (2020), The Southern Hemisphere Minor Sudden Stratospheric Warming in September 2019 and its Predictions in S2S Models, Journal of Geophysical Research: Atmospheres, 125(14), e2020JD032723.

Rayner, N. A., D. E. Parker, E. B. Horton, C. K. Folland, L. V. Alexander, D. P. Rowell, E. C. Kent, and A. Kaplan (2003), Global analyses of sea surface temperature, sea ice, and night marine air temperature since the late nineteenth century, Journal of Geophysical

436 Research: Atmospheres, 108(D14).
437 Reichler, T., J. Kim, E. Manzini, and J. Kröger (2012), A stratospheric connection to Atlantic
438 climate variability, Nature Geoscience, 5(11), 783-787.
439 Smith, K. L., and P. J. Kushner (2012), Linear interference and the initiation of extratropical
440 stratosphere-troposphere interactions, Journal of Geophysical Research: Atmospheres,
441 117(D13).
442 Straus, D. M., and J. Shukla (2000), Distinguishing between the SST-forced variability and
443 internal variability in mid-latitudes: Analysis of observations and GCM simulations, Quart.
444 J. Roy. Meteor. Soc., 126, 2323-2350.
445 Straus, D. M., and J. Shukla (2002), Does ENSO force the PNA?, J. Climate, 15, 2340-2358.
446 Wang, L., and W. Chen (2010), Downward Arctic Oscillation signal associated with moderate
447 weak stratospheric polar vortex and the cold December 2009, Geophysical Research
448 Letters, 37(9).
449 White, I. P., C. I. Garfinkel, J. Cohen, M. Jucker, and J. Rao (2021), The Impact of Split and
450 Displacement Sudden Stratospheric Warmings on the Troposphere, Journal of
451 Geophysical Research: Atmospheres, 126(8), e2020JD033989.
452 Xie, F., J. Li, W. Tian, J. Feng, and Y. Huo (2012), Signals of El Niño Modoki in the tropical
453 tropopause layer and stratosphere, Atmos. Chem. Phys., 12(11), 5259-5273.
454 Xie, F., X. Zhou, J. Li, C. Sun, J. Feng, and X. Ma (2018), The key role of background sea
455 surface temperature over the cold tongue in asymmetric responses of the Arctic
456 stratosphere to El Niño–Southern Oscillation, Environmental Research Letters, 13(11),
457 114007.

458 Zhang, J., W. Tian, M. P. Chipperfield, F. Xie, and J. Huang (2016), Persistent shift of the
459 Arctic polar vortex towards the Eurasian continent in recent decades, Nature Climate
460 Change, 6(12), 1094-1099.

461 **Tables**

462

463 **Table 1.** The correlation coefficients between different climate indices of interannual
464 (raw time series) and decadal (11-year moving averages) time scale. * one-tailed t-test
465 at the 90% significance level (** for 95%; *** for 99%).

466

Interannual	SST-PC1	SST-PC2	PWC1	PWC2	PNA	WP
PWC1	0.49***	0.51***	/	/	/	/
PWC2	0.37**	-0.34**	/	/	/	/
SSW1	0.38**	0.28**	0.58***	0.08	0.46***	0.33**
SSW2	-0.29**	-0.06	-0.34**	-0.21	-0.40**	-0.09

11yr	SST-PC1	SST-PC2	PWC1	PWC2	PNA	WP
PWC1	-0.2	0.71***	/	/	/	/
PWC2	0.52***	-0.22*	/	/	/	/
SSW1	-0.29**	0.76***	0.91***	-0.20	0.49***	0.69***
SSW2	-0.39***	-0.19	-0.52***	-0.23*	-0.55***	-0.16

467

468

Figures

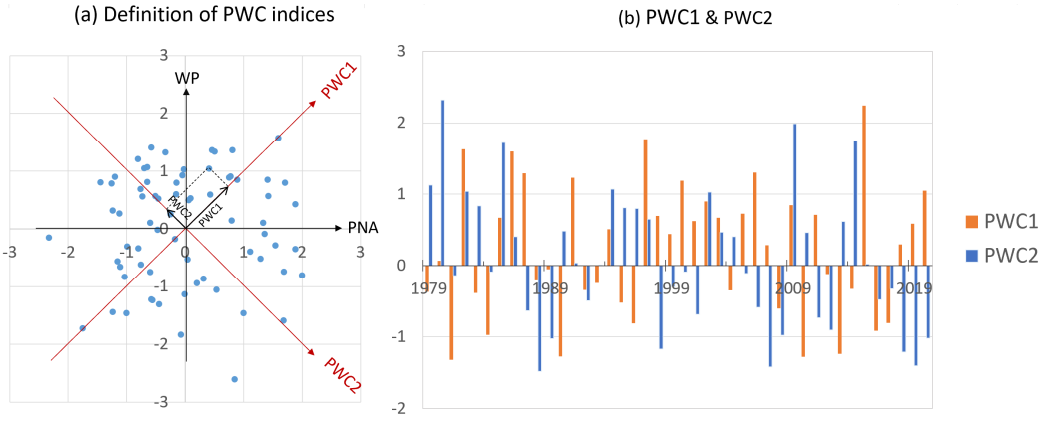

Figure 1 (a) The illustration of the definition of PNA and WP combined indices (PWC Index). (b) Time series of PWC1 and PWC2.

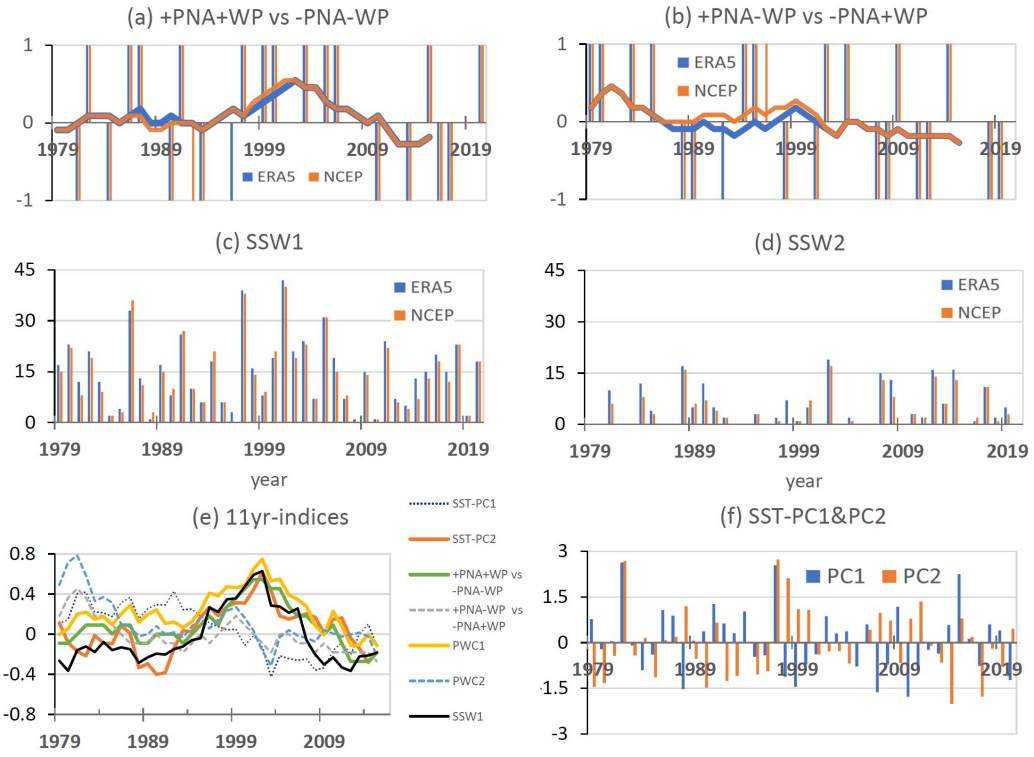

Figure 2 Time series from 1979 to 2020 of (a) +PNA+WP/−PNA−WP and (b) +PNA−WP/−PNA+WP. The duration (unit: day) of (c) SSW1 and (d) SSW2. (f) Two principal components of tropical Pacific SST. (e) 11-year moving averages of the climate indices from 1979 to 2015 (using the data from 1974 to 2020). The duration of SSW1 is normalized to compare with the moving averages of other indices.

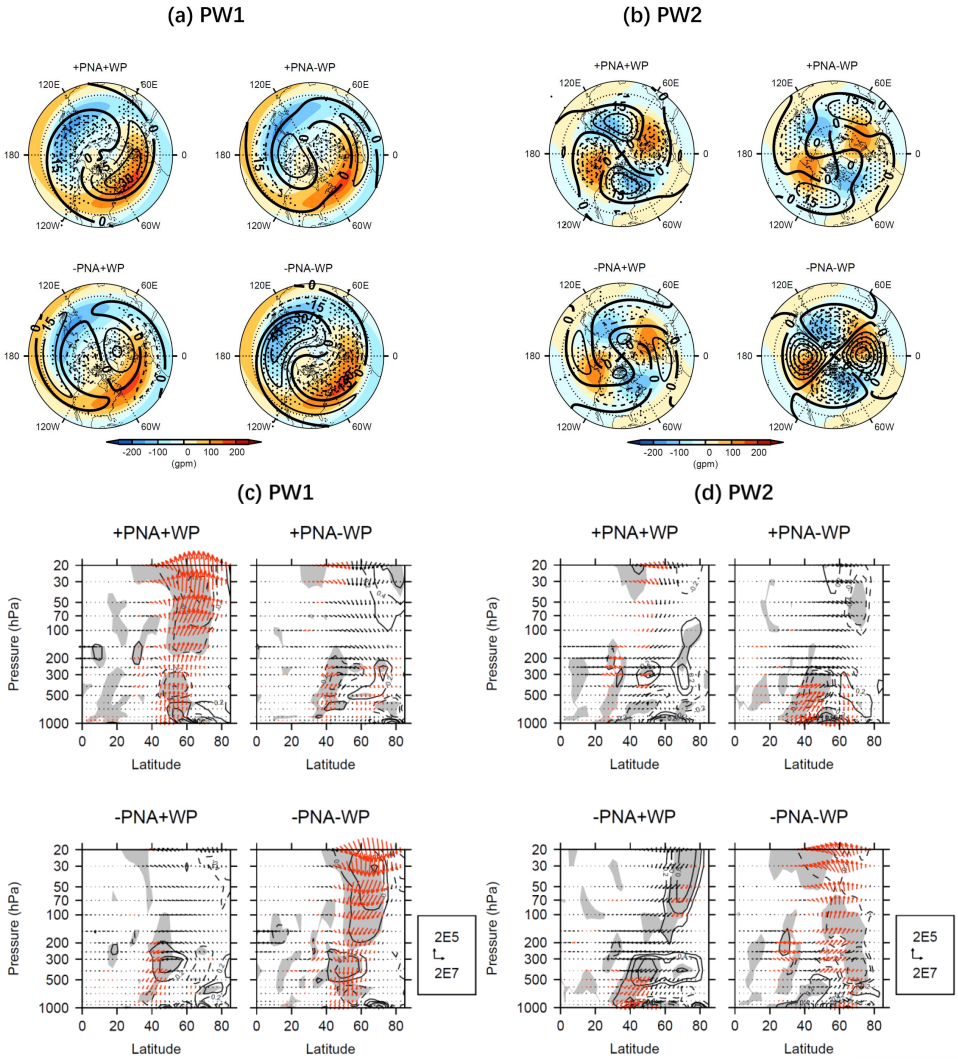

487

488

489 **Figure 3** (a) PW1 and (b) PW2 components of the geopotential height anomalies at

490 200 hPa (black contour lines with the intervals of ±15, ±30, ±45 gpm; color-filled

491 contours show the climatological mean) for different teleconnection combinations.

492 PW1 (c) and PW2 (d) components of the EP flux (unit: m^3s^{-2}) and EP flux divergence

493 (unit: $10^{-5}ms^{-2}$) anomalies. The regions of dots, red fluxes and grey divergence are

494 significant at the 95% confidence level according to Student's *t*-test.

495

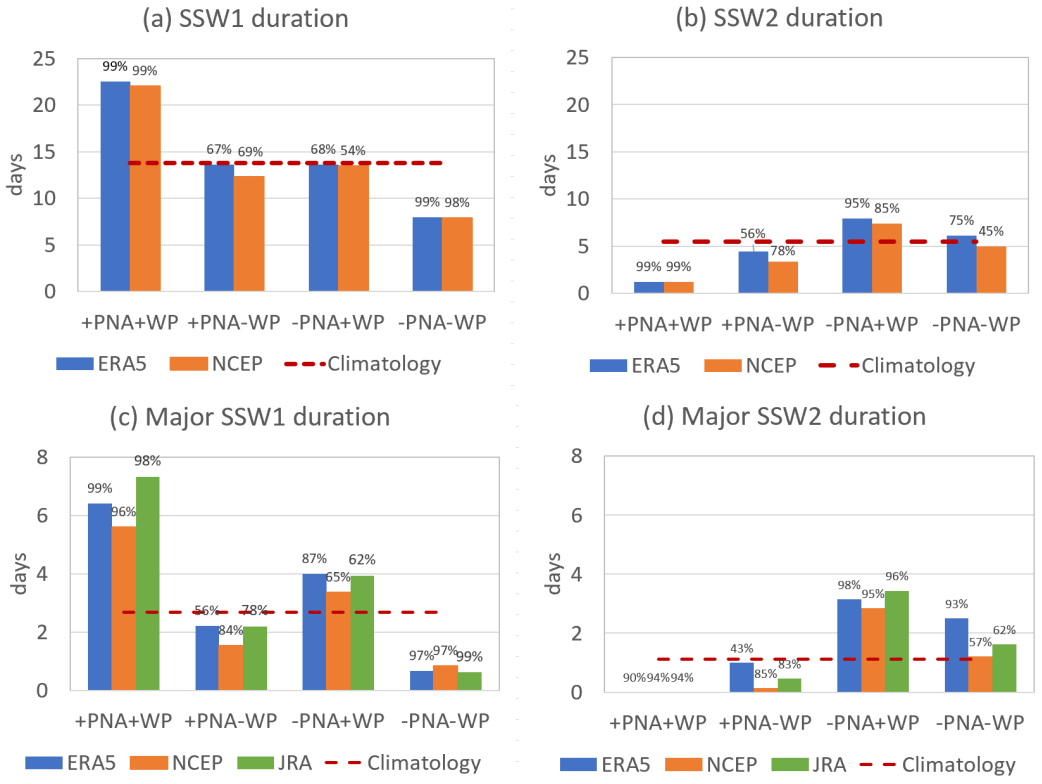

Figure 4 The duration of (a) SSW1, (b) SSW2, (c) major SSW1, and (d) major SSW2 corresponds to different combinations of the PNA and WP teleconnections. Monte Carlo test was used to calculate the statistical significance level of the deviations from climatology and the significance are labeled as percentage. Results of a and b are derived from ERA5 (1979-2020) and NCEP (1979-2020). Results of c and d are derived from ERA5(1950-2020), NCEP (1950-2020) and JRA55 (1958-2020).

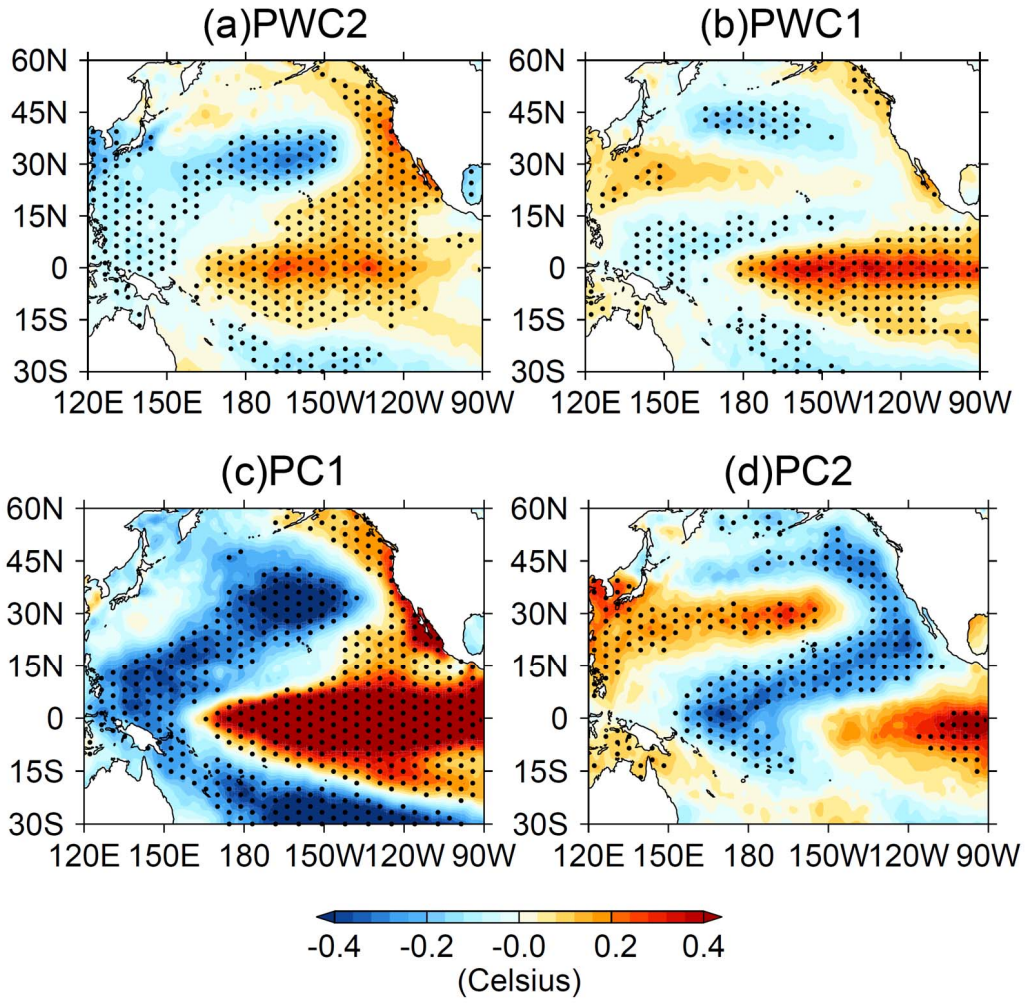

506

507 **Figure 5** The SST anomalies regressed to (a,b) PWC Index and (c,d) tropical Pacific

508 SST principal components. The regions of dots are significant at the 95% confidence

509 level according to the F-test.

510

Figure 1.

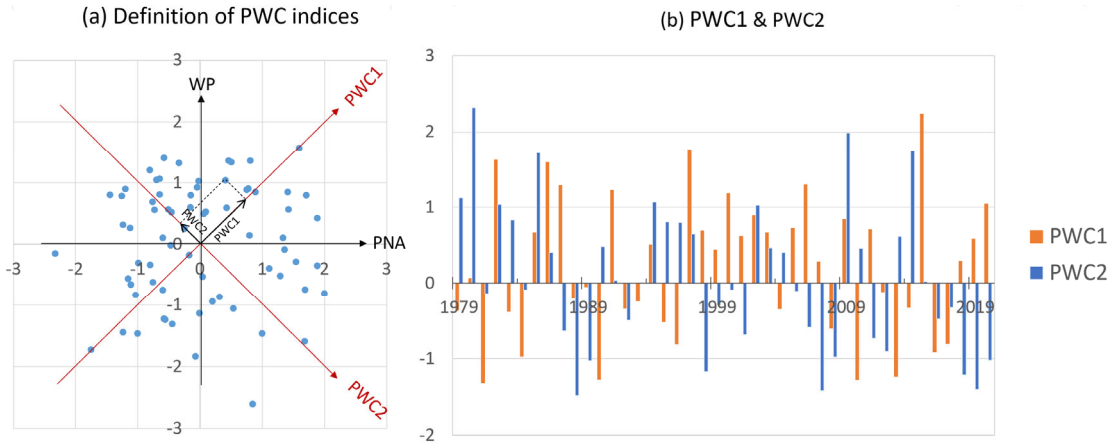
(a) Definition of PWC indices
WP
PNA
PWC1
PWC2
(b) PWC1 & PWC2
1979
1989
1999
2009
2019
PWC1
PWC2

Figure 2.

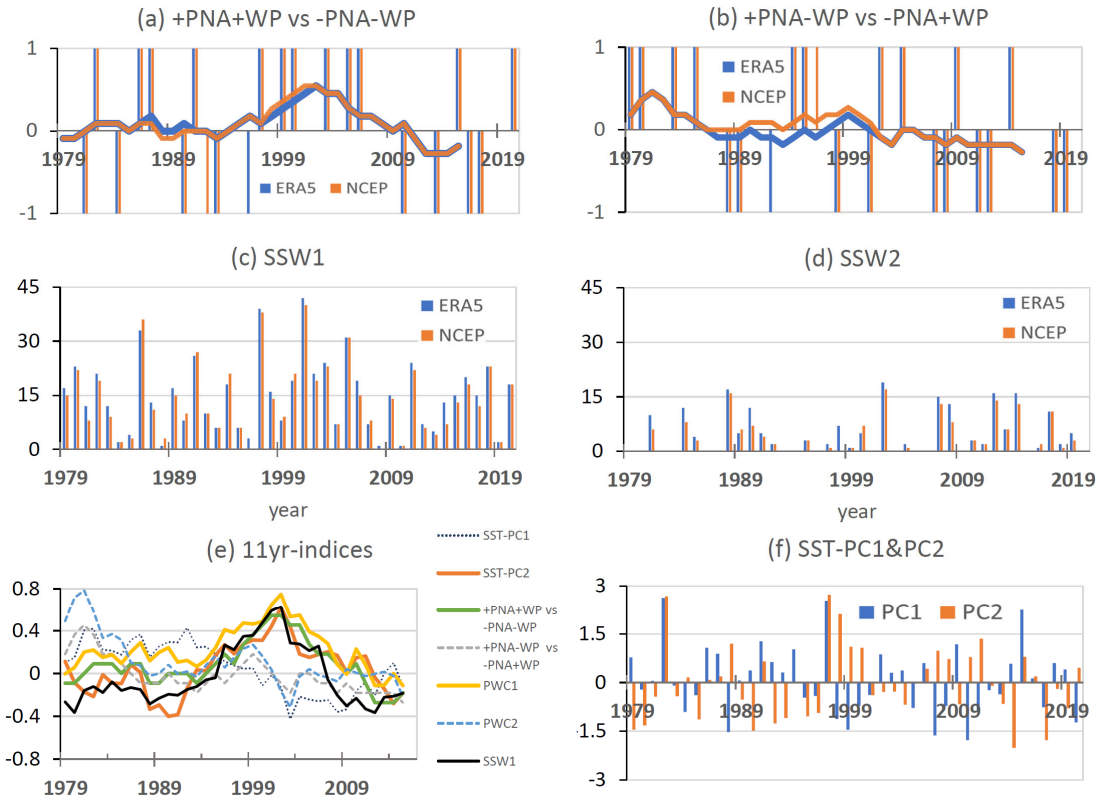
(a) +PNA+WP vs -PNA-WP
1
0
-1
1979
1989
1999
2009
2019
ERA5
NCEP
(b) +PNA-WP vs -PNA+WP
ERA5
NCEP
(c) SSW1
45
30
15
0
year
(d) SSW2
(e) 11yr-indices
0.8
0.4
-0.4
-0.8
SST-PC1
SST-PC2
+PNA+WP vs -PNA-WP
+PNA-WP vs -PNA+WP
PWC1
PWC2
SSW1
(f) SST-PC1&PC2
3
1.5
-1.5
-3
PC1
PC2

Figure 3.

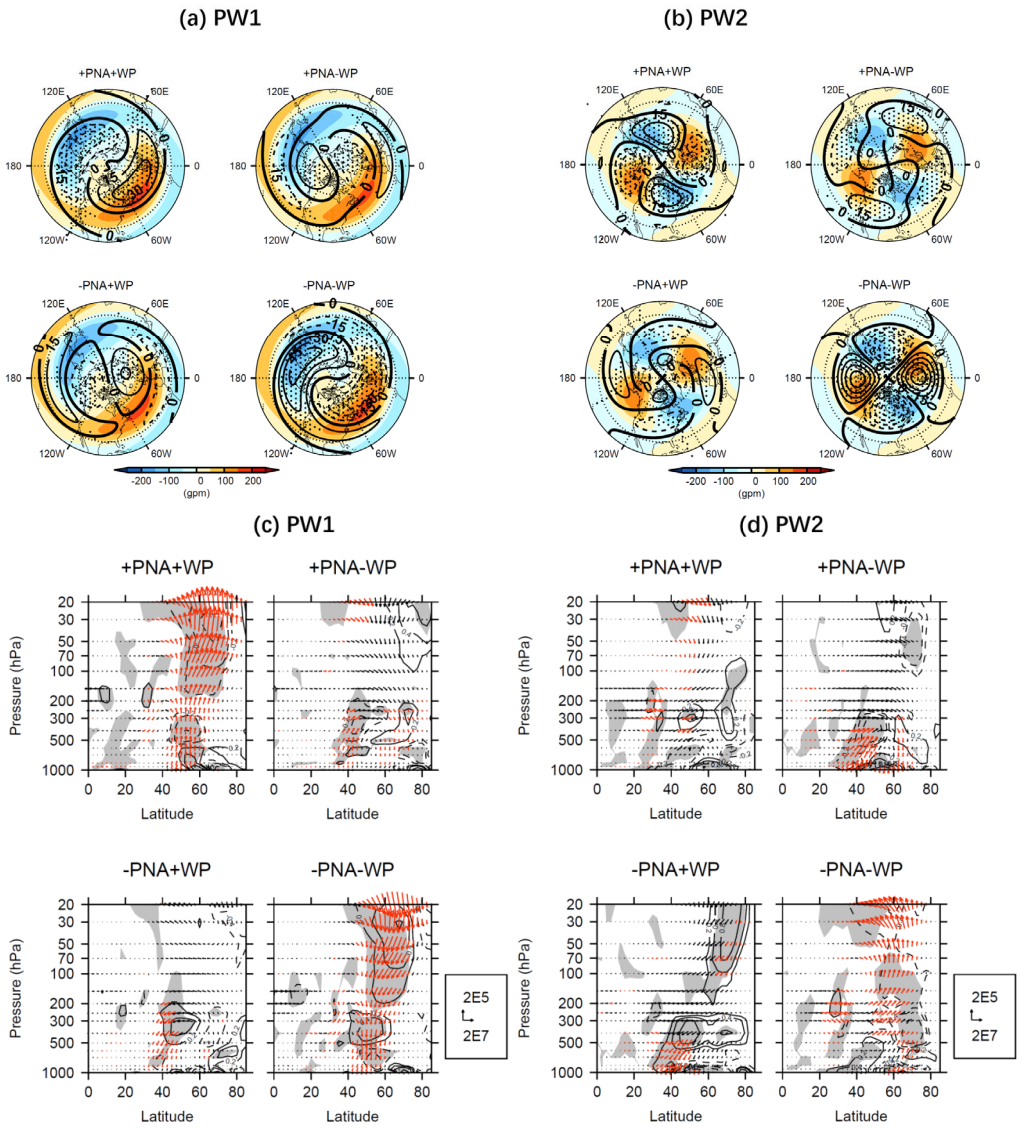
(a) PW1
(b) PW2
+PNA+WP
+PNA-WP
-PNA+WP
-PNA-WP
120E
60E
180
0
120W
60W
-200 -100 0 100 200
(gpm)
(c) PW1
(d) PW2
Pressure (hPa)
20
30
50
70
100
200
300
500
1000
0 20 40 60 80
Latitude
2E5
2E7

Figure 4.

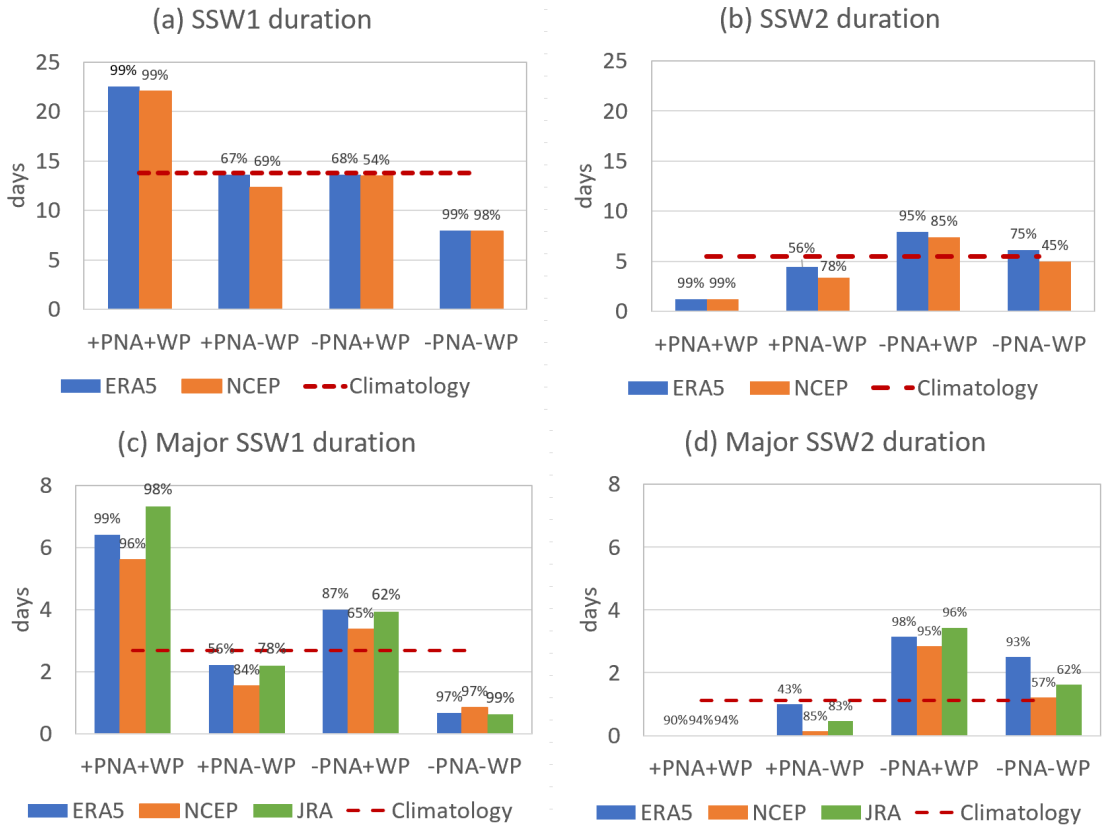
(a) SSW1 duration
days
25
20
15
10
5
0
99% 99%
67% 69%
68% 54%
99% 98%
+PNA+WP +PNA-WP -PNA+WP -PNA-WP
ERA5 NCEP Climatology
(b) SSW2 duration
days
99% 99%
56% 78%
95% 85%
75% 45%
+PNA+WP +PNA-WP -PNA+WP -PNA-WP
ERA5 NCEP Climatology
(c) Major SSW1 duration
days
8
6
4
2
0
99% 96% 98%
56% 84% 78%
87% 65% 62%
97% 97% 99%
+PNA+WP +PNA-WP -PNA+WP -PNA-WP
ERA5 NCEP JRA Climatology
(d) Major SSW2 duration
days
90% 94% 94%
43% 85% 83%
98% 95% 96%
93% 57% 62%
+PNA+WP +PNA-WP -PNA+WP -PNA-WP
ERA5 NCEP JRA Climatology

Figure 5.

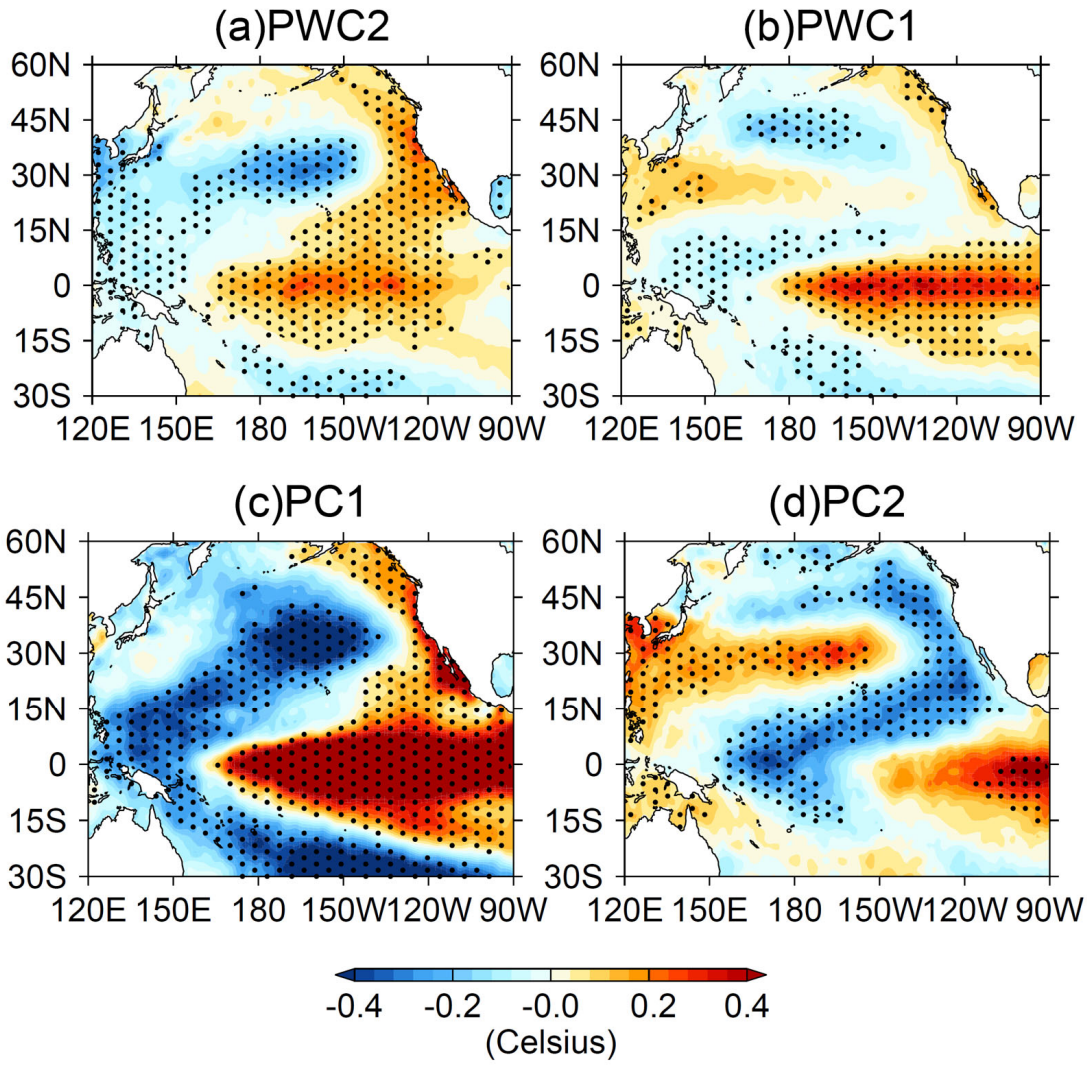
(a)PWC2
(b)PWC1
(c)PC1
(d)PC2
60N
45N
30N
15N
0
15S
30S
120E 150E 180 150W 120W 90W
-0.4 -0.2 -0.0 0.2 0.4
(Celsius)